Variability of the Fatigue Driving Force within Grains of Polycrystals

Gustavo M. Castelluccio[1,*], David L. McDowell[1,2]

[1] Woodruff School of Mechanical Engineering
2 School of Materials Science and Engineering
Georgia Institute of Technology, 771 Ferst Drive, N.W, Atlanta, Georgia 30332, USA
* Corresponding author: castellg@gatech.edu

Abstract Experimental studies in the last few decades have exhibited higher fatigue crack growth rates for cracks with size on the order of grains than would be predicted using growth laws based on LEFM. Small crystallographic fatigue cracks are affected by microstructure features that are not captured by traditional homogenous fracture mechanics theories (i.e., LEFM, EPFM). Since far-field driving force parameters cannot capture the intrinsic variability of the local fatigue driving force of small cracks induced by microstructure, alternative measures of the fatigue driving force are sought. This work employs finite element simulations that explicitly render the polycrystalline microstructure to compare nonlocal fatigue indicator parameters (FIPs) averaged over multiple volumes. The model employs a crystal plasticity algorithm in ABAQUS calibrated to study the effect of microstructure on early fatigue life of Ni-base RR1000 superalloy at elevated temperature under constant amplitude loading. The results indicate slight differences in the extreme values of distributions of FIPs for each element, slip plane cross-section (bands) and grain volumes. Furthermore, the grain average FIP better reflects the driving force for cracks on the cross section at the center of the grain while the extremes values of the FIPs averaged along bands tend to be located away from the grain centers.

Keywords Fatigue Indicator Parameter, Microstructurally Small Cracks, Fatigue Driving Force

1 Introduction

Extensive literature shows that fatigue experiments on metals in the high cycle fatigue (HCF) regime present variability in fatigue life of over a factor of 10. Multiple investigators have demonstrated that the underlying microstructural attributes [1][2] (i.e., grain size effects, elastic and plastic anisotropy, pre-existing defects) are usually responsible for the large variation in fatigue life. Indeed, in the HCF regime, the heterogeneous plastic deformation within favorably oriented and/or highly stressed grains controls the nucleation and early growth of fatigue cracks.

Recent finite element approaches that render the microstructure of metallic alloys have estimated the fatigue damage by assessing nonlocal fatigue indicator parameters (FIPs). These parameters typically refer to the value of the FIP averaged over certain mesoscale volumes (e.g., grain volumes). In contrast to local magnitudes within each finite element, these nonlocal FIPS mitigate effects of the mesh sensitivity and represent the physical length scale over which the fatigue damage occurs. Recent work [3][4] pursued definition of the averaging volume in terms of bands

that lie parallel to the crystallographic slip planes and have a width of one element. These bands seek to reflect domains in which cyclic plastic deformation localizes via dislocation dipole structures and in experimentally observed persistent slip bands.

By averaging the local FIPs over bands [3], a methodology was developed that predicts the path of a fatigue crack along bands through multiple grains, considering grain size effects [4]. The fact that FIPs can be averaged over multiple volumes (sizes and shapes) raises questions about the role of volume domains for averaging on the variability of nonlocal FIPs and the influence of grain size effects on the variance of the distribution of fatigue life.

This work employs a crystal plasticity finite element model for RR1000 Ni-base superalloy to compare the variability of the Fatemi-Socie FIPs averaged over grains or bands, and its local magnitudes for a number of realizations of ostensibly the same microstructure. The influence of grain size effects on normalized FIP distributions is also considered.

2 Modeling and simulation

2.1 Constitutive model

At the scale of individual grains we employ a physically-based crystal plasticity constitutive model for RR1000 superalloy adapted from the work of Lin et al. [5]. The crystallographic shearing rate is given by

$$\dot{\gamma}^{(\alpha)} = \dot{\gamma}_0 \exp\left[-\left(\frac{F_0}{k_b T}\right)\left\langle 1-\left\langle \frac{\left|\tau^{(\alpha)} - B^{(\alpha)}\right| - S^{(\alpha)}\mu/\mu_0}{\tau_0 \mu/\mu_0}\right\rangle^{p}\right\rangle^{q}\right] sgn\left(\tau^{(\alpha)} - B^{(\alpha)}\right), \quad (1)$$

in which $\dot{\gamma}^{(\alpha)}$ is the shearing rate of slip system α, $\tau^{(\alpha)}$ is the resolved shear stress, T is the absolute temperature, F_o, p, q, $\dot{\gamma}_0$, τ_0, μ, and μ_0 are material parameters that may differ for octahedral and cube slip systems, as listed in Table 1 for 650°C, and k_b is Boltzmann's constant. This formulation considers 12 octahedral and 6 cube slip systems, the latter representing a zigzag deformation mechanism [6] along octahedral planes, but producing net slip along cube planes. The model was implemented as a user-material subroutine (UMAT) in ABAQUS 6.9 [7] using an implicit integration scheme based on the Newton-Raphson and the backward-Euler methods. Discussion of model parameters and their estimation can be found in Ref. [8].

The slip system shearing rate relation includes a directional slip resistance $S^{(\alpha)}$ that functions as a theshold stress below which no plastic flow occurs and a back stress $B^{(\alpha)}$ that accounts for directional hardening (Bauschinger effects) on the slip system. The evolution laws for slip resistance and back stress are written as

$$\dot{S}^{(\alpha)} = \left[h_S - d_D\left(S^{(\alpha)} - S_0^{(\alpha)}\right)\right]\left|\dot{\gamma}^{(\alpha)}\right| \quad (2)$$

$$\dot{B}^{(\alpha)} = h_B \dot{\gamma}^{(\alpha)} - r_D^{(\alpha)} B^{(\alpha)} \left| \dot{\gamma}^{(\alpha)} \right|, \tag{3}$$

in which $r_D^{(\alpha)} = \frac{h_B \mu_0}{S^{(\alpha)}} \left\{ \frac{\mu_0'}{f_c \lambda} - \mu \right\}^{-1}$ and S_0, h_B, h_S, d_D, μ_0', f_c, λ, are constants that differ for octahedral and cube slip planes (see Table 1). Both evolution equations follow a hardening-dynamic recovery format and the initial values are specified as S_0 for the slip resistance and zero for the back stress.

Table 1. Parameters of the constitutive model at 650°C for octahedral and cube slip systems.

	F_0 kJ/mol	p	Q	$\dot{\gamma}_0 s^{-1}$	τ_0 *GPa*	S_0 *MPa*	f_c	h_B *GPa*	h_S *GPa*	d_D *MPa*	μ'_0 *GPa*
Oct.	295	0.31	1.8	120	810	350	0.42	400	10	6024	72.3
Cube	295	0.99	1.6	4	630	48	0.18	100	4.5	24	28.6

Other parameters: λ=0.85, μ_0= 192GPa.
Elastic constants: C_{11} = 166.2GPa, C_{12} = 66.3GPa, C_{44} = 138.2GPa.

2.2 Simulations

Figure 1 depicts a mesh composed of "brick" elements (C3D8R) employed for modeling smooth specimens, containing 6859 elements and 118 grains, with colors representing different crystallographic orientations. The loading sequence consisted of relative displacement of the upper and lower boundary planes at a 0.05%/s strain rate under tensile mode loading to achieve overall nominal peak strains of 0.8% and strain ratio (R_ε) equal to zero, typical of the HCF regime. The lateral faces are free of traction and the model has unidirectional periodic boundary conditions along the loading direction (Y-axis) such that the sum of the displacement perturbations of the nodes on top and bottom faces relative to the mean is null, leaving only the imposed net relative displacement. The grain size follows a lognormal distribution based on the algorithm by Musinski [9] and has a mean grain size about 18 μm.

2.3 Fatigue driving force measures

Since the local driving force to nucleate and grow fatigue cracks is affected by the microstructure, several FIPs have been proposed to consider these effects. Fatemi and Socie [10] proposed a FIP based on the critical plane approach that plays a role similar to that of the mixed mode ΔCTD or ΔJ-integral in correlating with growth of small fatigue cracks [11][12][13]. Subsequently, several investigators have successfully employed approaches akin to such FIP along with crystal plasticity formulations for studying the effects of microstructure on fatigue crack formation and early growth within the first few grains [14][15][16].

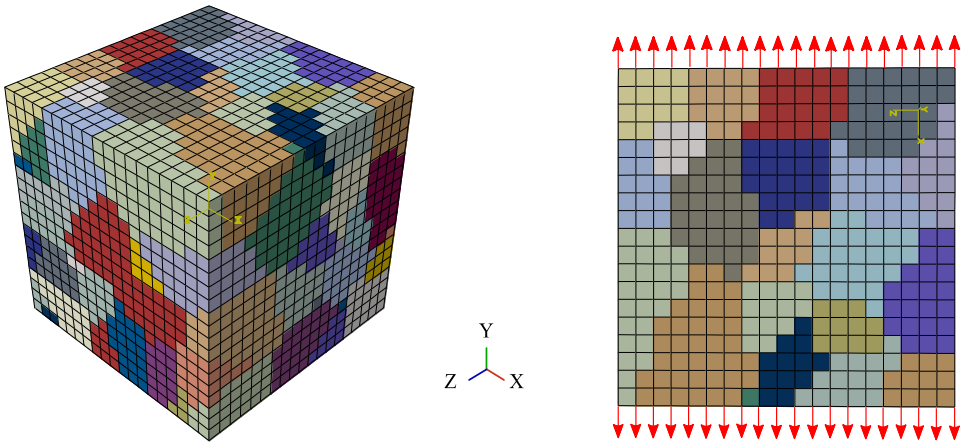

Figure 1. Example of a mesh with the explicit microstructure for axial loading of smooth specimens. Quasistatic mean relative displacement of the upper and lower boundary planes is depicted by the red arrows.

Castelluccio and McDowell [3] proposed to quantify the driving force for transgranular failure with a crystallographic version of the Fatemi-Socie FIP defined for each octahedral slip system, i.e.,

$$\mathrm{FIP}^{\alpha} = \frac{\Delta\gamma_p^{\alpha}}{2}\left(1 + k\frac{\sigma_n^{\alpha}}{\sigma_y}\right) \tag{4}$$

where $\Delta\gamma_p^{\alpha}$ is the cyclic plastic shear strain range on slip system α, σ_n^{α} is the peak stress normal to this slip system, σ_y is the cyclic uniaxial yield strength of the polycrystal, and $k = 1$, as proposed by Fatemi and Socie [10]. The algorithm computes the FIP on each slip system and for each element using the range of plastic strain over the third loading cycle [3]. This methodology allows for an approximate stress redistribution to almost represent "steady state" cyclic conditions in terms of stress and plastic strain redistribution within the polycrystal in the HCF regime, since the microstructure exerts a dominant influence on the transient cyclic plastic deformation fields.

2.3.1 Mesoscale averaging volumes for FIPs

To numerically regularize the FEM discretization and also to represent the finite physical scale of the fatigue damage process zone, the FIPs calculated at each integration point in the mesh are averaged over a selected mesoscale volume. In the present approach we consider three volumes (Figure 2): (i) individual elements, (ii) bands parallel to slip planes, and (iii) entire grain volume. Figure 2 presents a cluster of finite elements that form one grain. Each grain is subdivided in bands of one element of width that are parallel to slip planes as described in Refs. [3][4][8]. The nonlocal FIP is averaged separately over each of these volumes—elements, bands and grains.

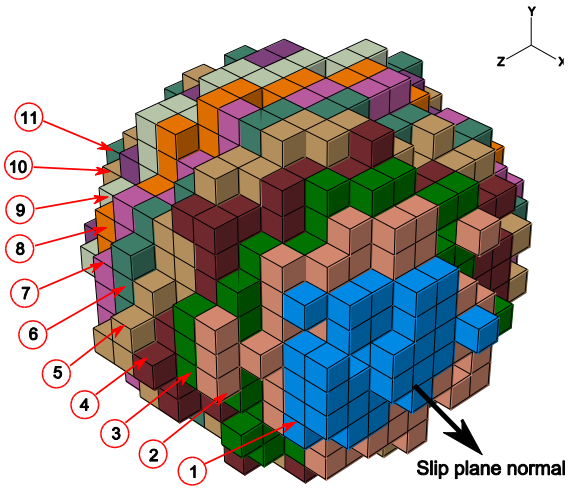

Figure 2: Schematic representation of elements, bands and grains in which FIPs are averaged to estimate transgranular fatigue crack growth. The implementation in a FEM model with unstructured, voxellated meshing is shown, with bands color coded and numbered for a single spherical grain.

3 Assessment of non-local FIP averaging volumes

A total of 50 equivalent realizations with random grain distributions for nominally the same microstructure with mean grain size of about 18 μm were utilized to compare the FIP averaged over grains (FIP_{grains}), bands (FIP_{band}), or the local FIP on every element ($FIP_{element}$). In each case, the average is computed for each octahedral slip system over the corresponding domain.

Figure 3 presents the distributions of the FIP for each element ($FIP_{element}$) and the averages over bands (FIP_{band}) and grains (FIP_{grains}) compiled from 50 equivalent realizations considering all the octahedral slip systems. Since fatigue life is dominated by the extreme distributions, these results consider only values larger than FIP_{thresh} =MAX(FIP_{grains})/1000. The three cases present similar distributions and the extreme value of the three distributions lie between $2x10^{-3}$ and $3x10^{-3}$. Since elements are smaller than the grain scale, the FIPs averaged over elements have somewhat higher extreme values than either grain- or band-averaged FIPs.

Figure 4 presents the distributions of band-averaged FIPs that result from dividing the grain into seven regions, each aligned along slip planes which are oriented perpendicular to the slip plane normal. Note that the number of bands per grain is not constant, so each region may include more than one band from a single grain and slip system. The FIP_{band} presents similar distributions from all sections of the grains, which suggests that there is no dependence of the FIPs on the section from which it belongs (e.g., closer to the center of the grain).

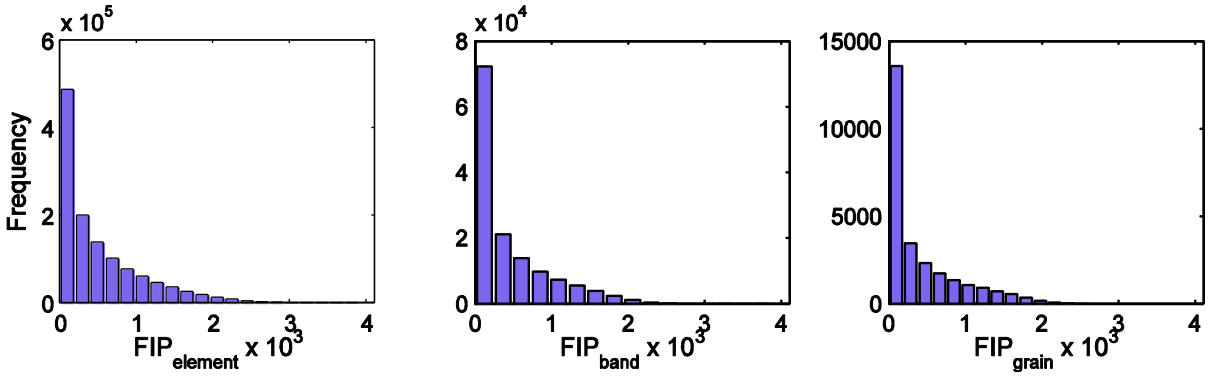

Figure 3. Distributions of the FIP from each element, band and grain for values larger than FIP_{thresh} from 50 equivalent realizations.

To assess the difference between averaging over bands or grains, Figure 5 presents a series of histograms with ratio FIP_{band}/FIP_{grain}; such ratios are presented in a semi-log scale between 0.1 and 10 only considering FIP values larger than FIP_{thresh} for bands or grains. Furthermore, we classified the histograms with the sections from which they belong (rows 1 to 7) or the range of the FIP_{grain} (columns, the FIP increases to the right).

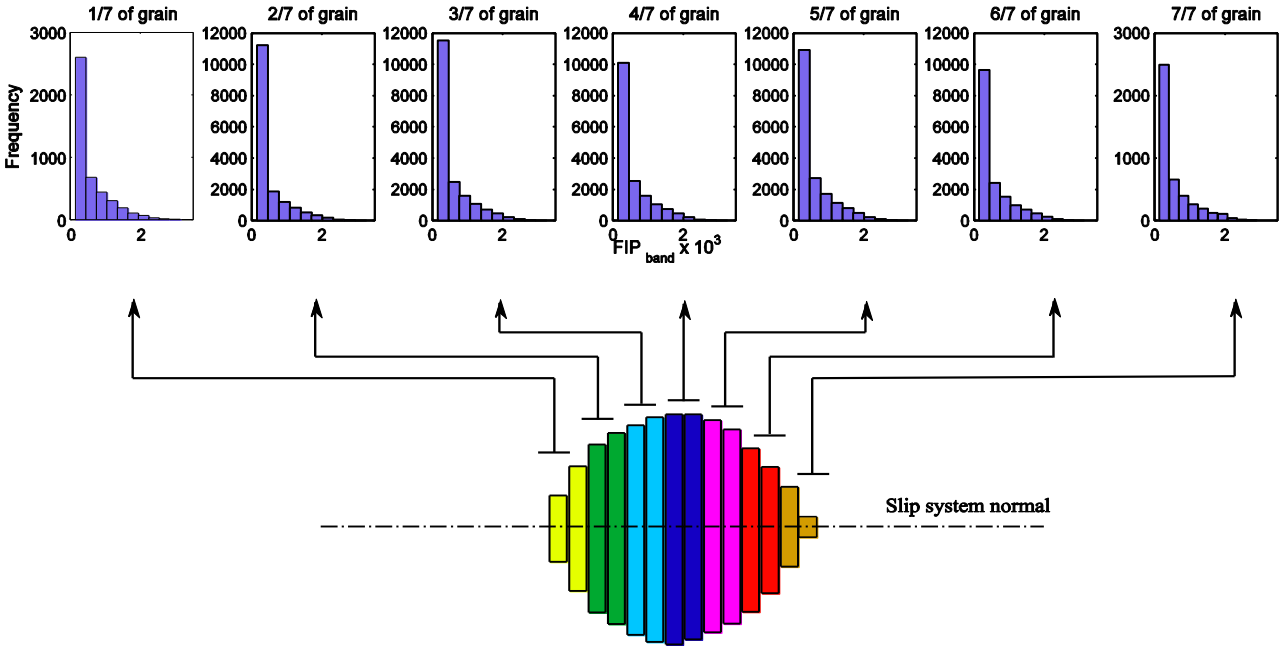

Figure 4. FIP_{band} distributions classified by the region they occupy within a grain, computed from 50 realizations. Only values larger than FIP_{thresh} are considered.

The results show that the variability of the ratio FIP_{band}/FIP_{grain} decreases both towards larger FIPs and the center of the grain. Therefore, the average of the FIP over the entire grain closely mimics the FIP computed at the center cross section of the grain for large values of FIPs.

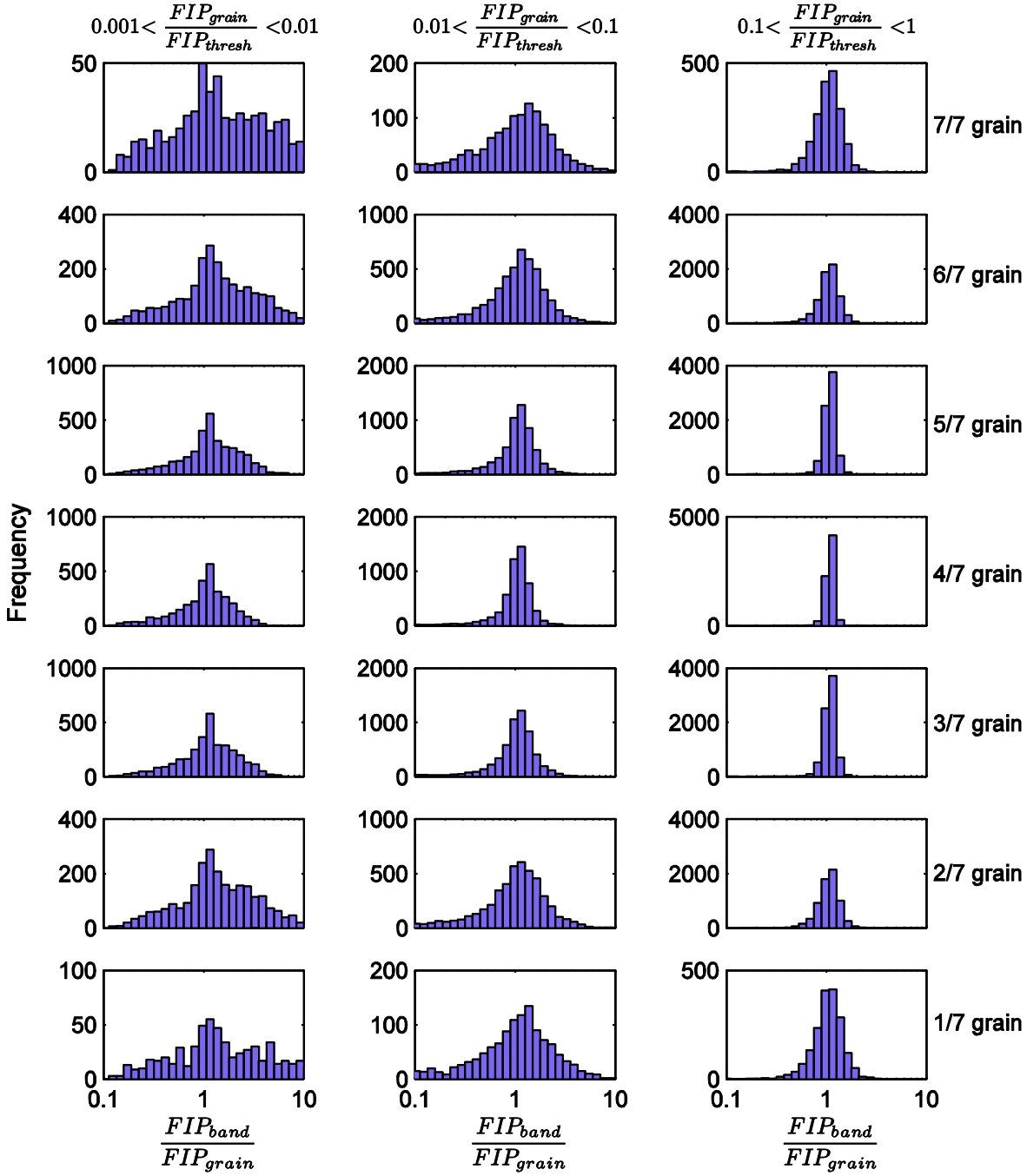

Figure 5. Distributions of the ratio between FIP_{band} and FIP_{grain}, classified by region they occupy in the grain (rows) and the intensity of the FIP_{band} and FIP_{grain} (columns).

3.1 Grain size effects

Grain size effects on fatigue crack formation and early transgranular growth have been modeled by

introducing a dependence of plastic deformation (or the FIP) on the grain size. Such a definition can be ambiguous since the "cross sectional area of the grain" differs for each slip plane that cuts through it. For example, the grain size can be computed for each band as the square root of the cross sectional area or as the diameter of a spherical grain with equivalent volume. Figure 6 presents the distributions of the size of the bands (scales as the square root of the number of elements within) and grains (scales as the cubic root of the number of elements within) normalized by the reference grain size (d_{gr}^{ref} =18μm.); the distributions are clearly different, with the same extreme values but a lower mean value for the band size distribution. In previous work [3][8] we have estimated the fatigue life to nucleate a crack by assuming a proportional dependence of the FIP on the normalized grain size, d_{gr}, (either the size of the band or the diameter of the grains) described by

$$A = d_{gr} \Big/ d_{gr}^{ref} \tag{5}$$

By multiplying A by the FIP we obtain the normalized driving force

$$A \cdot FIP = d_{gr} \Big/ d_{gr}^{ref} \; FIP \tag{6}$$

Distributions in Figure 7 present normalized values of $A \cdot FIP$. It is noted that, because the extreme values associated with FIP_{band} do not tend to be associated with the center of grains, the cross sectional dimension of their associated planes is usually smaller than the grain diameter based the cube root of the grain volume. Accordingly, the distributions of $A \cdot FIP_{band}$ and $A \cdot FIP_{grain}$ are very similar. However, the maximum extreme values of the grain-averaged FIPs are somewhat higher.

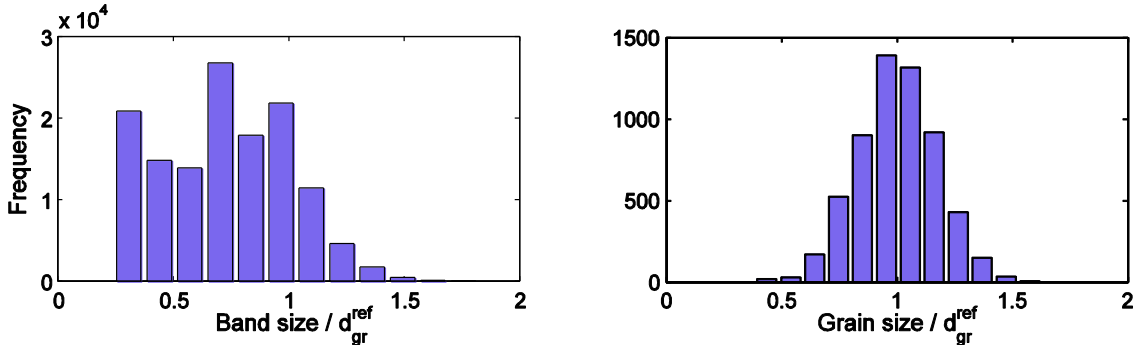

Figure 6. Distributions of the normalized size of bands (left) and grains (right).

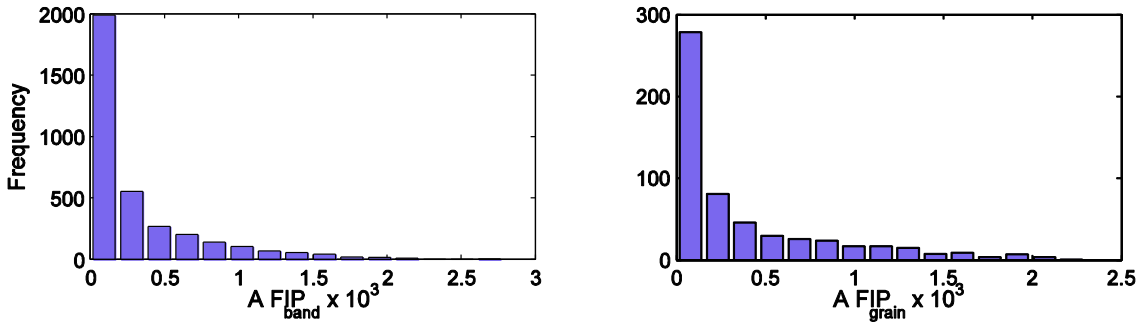

Figure 7. Distributions of the FIPs regularized with the grain size effects for bands, FIP_{band}, (left) and grains, FIP_{grain}, (right).

4 Conclusions

Results of this work support the following conclusions:

- The distributions of FIPs for each element, slip plane cross-section (bands) and the grain volume are very similar with only slight differences in the extreme values.
- Grain averages of FIP represents better the largest cross section representative of the center of the grain.
- The extremes values of the FIPs averaged along the slip plane cross-sectional area tend to be located away from the center of the grains.
- The methodology employed to define grain size effects can affect the variability of the fatigue driving force and modify the distribution of extreme FIP values.

Acknowledgements

G. M. Castelluccio and D.L. McDowell are deeply grateful for the support provided by Integrated Systems Solutions, Inc. (Technical Monitor: Dr. Nam Phan, NAVAIR).

References

[1] K. Gall, H. Sehitoglu, and Y. Kadioglu, 'A Methodology for Predicting Variability in Microstructurally Short Fatigue Crack Growth Rates', *J. Eng. Mater. Technol.*, vol. 119, no. 2, pp. 171–179, 1997.

[2] V. P. Bennett and D. L. McDowell, 'Polycrystal orientation distribution effects on microslip in high cycle fatigue', *Int J. Fatigue*, vol. 25, no. 1, pp. 27–39, Jan. 2003.

[3] G. Castelluccio, D. L. McDowell, 2013 Effect of annealing twins on crack initiation under high cycle fatigue conditions. *J.Mater. Sci.*, 48, 2376-2387, 2013.

[4] G. Castelluccio, D. L. McDowell, 'Fatigue Life Prediction of Microstructures'. In *Proceedings of the ASME International Mechanical Engineering Congress and Exposition*. Houston, Texas, USA: ASME, 2012.

[5] B. Lin, L. G. Zhao, J. Tong, and H.-J. Christ, 'Crystal plasticity modeling of cyclic deformation for a polycrystalline nickel-based superalloy at high temperature,' *Mater. Sci. Eng., A*, 527(15), 3581–3587, 2010.

[6] W. Österle, D. Bettge, B. Fedelich, and H. Klingelhöffer, 'Modelling the orientation and

direction dependence of the critical resolved shear stress of nickel-base superalloy single crystals', *Acta Mater.*, vol. 48, no. 3, pp. 689–700, Feb. 2000.

[7] ABAQUS, *FEM software V6.9, Simulia Corp., Providence, RI, USA*. Providence, RI, USA: Simulia, Inc., 2009.

[8] G. M. Castelluccio, 'A study on the influence of microstructure on small fatigue cracks', PhD Thesis, Georgia Institute of Technology, Atlanta, GA, USA, 2012.

[9] W. D. Musinski, D. L. McDowell, Microstructure-sensitive probabilistic modeling of HCF crack initiation and early crack growth in Ni-base superalloy IN100 notched components. *Int. J. Fatigue*, 37, 41–53, 2012.

[10] A. Fatemi, D. F. Socie, D. F., 1988. A critical plane approach to multiaxial fatigue damage including out-of-phase loading. *Fatigue Fract. Eng. Mater. Struct.*, 11(3), 149—165.

[11] S. C. Reddy and A. Fatemi, 'Small Crack Growth in Multiaxial Fatigue', in *Advances in Fatigue Lifetime Predictive Techniques*, ASTM, 1992, pp. 276–298.

[12] D. L. McDowell and J. Y. Berard, 'A ΔJ-based approach to Biaxial Fatigue', *Fatigue Fract. Eng. Mater. Struct.*, vol. 15, no. 8, pp. 719–741, 1992.

[13] G. M. Castelluccio and McDowell D. L., "Assessment of Small Fatigue Crack Growth Driving Forces in Single Crystals with and without Slip Bands, *Int. J. Fatigue*, 176(1) (2012): 49-64.

[14] K. Kirane, S. Ghosh, M. Groeber, and A. Bhattacharjee, 'Grain Level Dwell Fatigue Crack Nucleation Model for Ti Alloys Using Crystal Plasticity Finite Element Analysis', *J. Eng. Mater. Technol.*, vol. 131, no. 2, pp. 021003 1–14, 2009.

[15] C. Przybyla, R. Prasannavenkatesan, N. Salajegheh, and D. L. McDowell, 'Microstructure-sensitive modeling of high cycle fatigue', *Int. J. Fatigue*, vol. 32, no. 3, pp. 512–525, 2010.

[16] M. M. Shenoy, J. Zhang, and D. L. McDowell, 'Estimating fatigue sensitivity to polycrystalline Ni-base superalloy microstructures using a computational approach', *Fatigue Fract. Eng. Mater. Struct.*, vol. 30, no. 10, pp. 889–904, 2007.